

DRC FILE COPY

Technical
Memorandum 88-16

Defence Research
Establishment Pacific

Centre de recherches
pour la défense pacifique

(3)



AD-A202 983

OSRMS: The DREP Near-Nadir Scatterometer

L.C. Rempel, B.A. Hughes and S.J. Hughes

August 1988

DTIC
ELECTED
DEC 07 1988
S D
H

**BEST
AVAILABLE COPY**

Research and Development Branch
Department of National Defence

Canada

DISTRIBUTION STATEMENT A
Approved for public release;
Distribution Unlimited

88 12 7 007



Defence Research
Establishment Pacific

Centre de recherches
pour la défense pacifique

TECHNICAL MEMORANDUM 88-15

DEFENCE RESEARCH ESTABLISHMENT PACIFIC

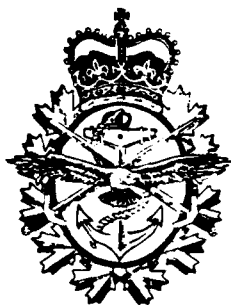
CFB Esquimalt, FMO Victoria, B.C. V0S 1BO

OSRMS: THE DREP NEAR-NADIR SCATTEROMETER

by

L.C. Rempel, B.A. Hughes and S.J. Hughes

August 1988



Approved by:

T. J. Smith

CHIEF

Research and Development Branch
Department of National Defence

Canada

Abstract

The ocean surface roughness measurement system (OSRMS) is a near-nadir-directed infrared (IR) scatterometer specially constructed for and operated by the Defence Research Establishment Pacific (DREP). It has been used to measure ocean-surface parameters and particularly for the examination from an aircraft of internal waves.

This paper gives a description of the configuration and operation of the OSRMS including the mechanical, electrical, electronic, optical and software components. A brief overview of the trials in which the OSRMS took part is included, with the main focus on the 1987 trial, SCATMOD III and the data obtained in that trial. The discussion of the data from this trial contains examples of internal waves, ship wakes, and aircraft attitude compensation, and a description of wind velocity effects on the speckle noise.



| Accession For | |
|--------------------|-------------------------------------|
| NTIS CRA&I | <input checked="" type="checkbox"/> |
| DTIC TAB | <input type="checkbox"/> |
| Characterized | <input type="checkbox"/> |
| Justified | <input type="checkbox"/> |
| By _____ | |
| Distribution _____ | |
| Available by _____ | |
| Dist _____ | |
| A-1 | |

Table of Contents

| | <u>Page</u> |
|----------------------------------|-------------|
| Abstract | iii |
| List of Figures | vii |
| List of Tables | ix |
| 1. Introduction | 1 |
| 2. System Overview | 2 |
| 3. OSRMS Description | 4 |
| a) Mounting | 4 |
| b) Electrical Requirements | 5 |
| c) Electronics | 5 |
| Scan mirror control | 5 |
| Computer interface | 7 |
| Mirror sweep generator | 7 |
| Scan-mirror pitch control | 9 |
| Scan-mirror roll control | 9 |
| Laser fire control timing | 9 |
| Receiver card | 10 |
| d) Computer System | 11 |
| e) Laser | 12 |
| Laser cooling | 14 |
| Beam specifications | 14 |
| 4. Review of Trials | 18 |
| a) Overview | 18 |
| JOWIP | 18 |
| SARSEX | 18 |
| SCATTMOD II | 19 |
| SCATTMOD III | 19 |
| b) Data from SCATTMOD III | 19 |
| 5. Conclusions | 32 |
| REFERENCES | 34 |

List of Figures

| | <u>Page</u> |
|--|-------------|
| 1. Block Diagram of OSRMS..... | 3 |
| 2. OSRMS Scan Pattern..... | 6 |
| 3. Scan-Mirror Drive Waveforms..... | 8 |
| 4. OSRMS Optical System Components..... | 12 |
| 5. Optical System Layout..... | 13 |
| 6. Beam Area Versus Drive Current..... | 16 |
| 7. Example of OSRMS imagery taken on 1987 Aug 17, 11:32h to 11:35h at 48°45'N, 126°45'W..... | 21 |
| 8. Example of OSRMS imagery taken on 1987 Aug 18, 11:12h to 11:15h at 48°16.9'N, 126°45'W..... | 22 |
| 9. Example of OSRMS imagery taken on 1987 Aug 19, 12:05h to 12:08h at 48°45'N, 126°45'W..... | 23 |
| 10. OSRMS image showing internal wave modulation..... | 25 |
| 11. OSRMS image showing the wake of the freighter FRUITION..... | 26 |
| 12. Examples of undocumented shipwakes taken on 1987 Aug 17, 16:13h to 16:16h at 48°45'N, 126°45'W..... | 27 |
| 13. Imagery showing effect of roll compensation..... | 29 |
| 14. Beam angle versus roll ramp..... | 30 |
| 15. OSRMS noise standard error as function of windspeed and direction..... | 31 |

List of Tables

| | <u>Page</u> |
|--|-------------|
| 1. Beam size versus laser current..... | 15 |
| 2. Beam area versus laser current..... | 17 |
| 3. Summary log of SCATTMOD III runs..... | 20 |

1. Introduction

The ocean surface roughness measurement system (OSRMS) is a near-nadir-directed infrared (IR) scatterometer specially constructed for and operated by the Defence Research Establishment Pacific (DREP). It was designed to evaluate the concept of using optical energy reflected from the ocean's surface as a means of measuring internal waves with wavelengths between 100 and 1000 metres. The subsurface currents associated with the internal waves modulate ocean surface waves producing alternating bands of increased and decreased roughness. For a collimated optical beam incident on a rough surface the amount of radiation reflected in a specific direction is proportional to the amount of illuminated surface having the appropriate reflecting slope angle. The latter amount is taken to be a direct basic measurement of surface roughness. Relative roughness variations can be obtained by comparing the relative values of received energy from contiguous spots covering a sufficiently large area.

It was determined in preliminary studies¹ by Spar Aerospace Limited (SPAR) for DREP that within the constraints of operating on a Convair-580 aircraft, and for experimental purposes, an IR laser system at a wavelength of 1.06 micrometres would be suitable. This frequency puts a limitation on the weather conditions since infrared is attenuated and scattered by aerosols and water vapour, and particularly by clouds. Lower frequencies have a higher transmission through cloud but require larger and more complicated transmitters and receivers.

It was also decided that the system would use discrete spots with a diameter of ten metres to trace out a swath a thousand metres wide on the ocean surface beneath the aircraft. This spot size is much larger than the local roughness dimensions, so it provides some statistical smoothing, but is small relative to the wavelength of the internal waves being measured.

Based upon its preliminary studies, SPAR developed and constructed the OSRMS which has been used in a number of experiments by DREP. This paper describes the system and reviews the experiments.

2. System Overview

Figure 1 shows a block diagram of the OSRMS. The power requirement of each block is indicated where applicable.

The aircraft signals include navigational information: longitude, latitude, heading, altitude, ground speed, pitch, and roll, which are read into the OSRMS computer. Ground speed, pitch, and roll are forwarded to the OSRMS controller which uses this information for scan-mirror positioning and laser-fire timing to ensure that the swath is in the proper location on the ocean surface beneath the aircraft. The controller triggers the laser to fire when the scan mirror is in the correct position. The amplitude of the outgoing IR pulse is sensed by a photodiode at the back of the laser and returned to the controller as the "transmitted signal". The main infrared pulse emitted from the front of the laser head is directed to the scan mirror which reflects the beam through a window in the underside of the aircraft fuselage down to the ocean surface.

The energy reflected from the ocean surface that intercepts the scan mirror is directed back to the receiver avalanche photodiode (APD), amplified in the preamplifier, and sent to the controller. The controller converts the peak value of this "received signal" and that of the "transmitted signal" to digital quantities and transmits them to the computer.

The computer displays the matrix of signal amplitudes as intensities on a graphics screen so that the data can be seen in real time in the format of a swath equivalent to the one being traced out on the ocean surface. The computer display also shows navigational data and other relevant information. The data are recorded on magnetic tape together with some of the navigational data.

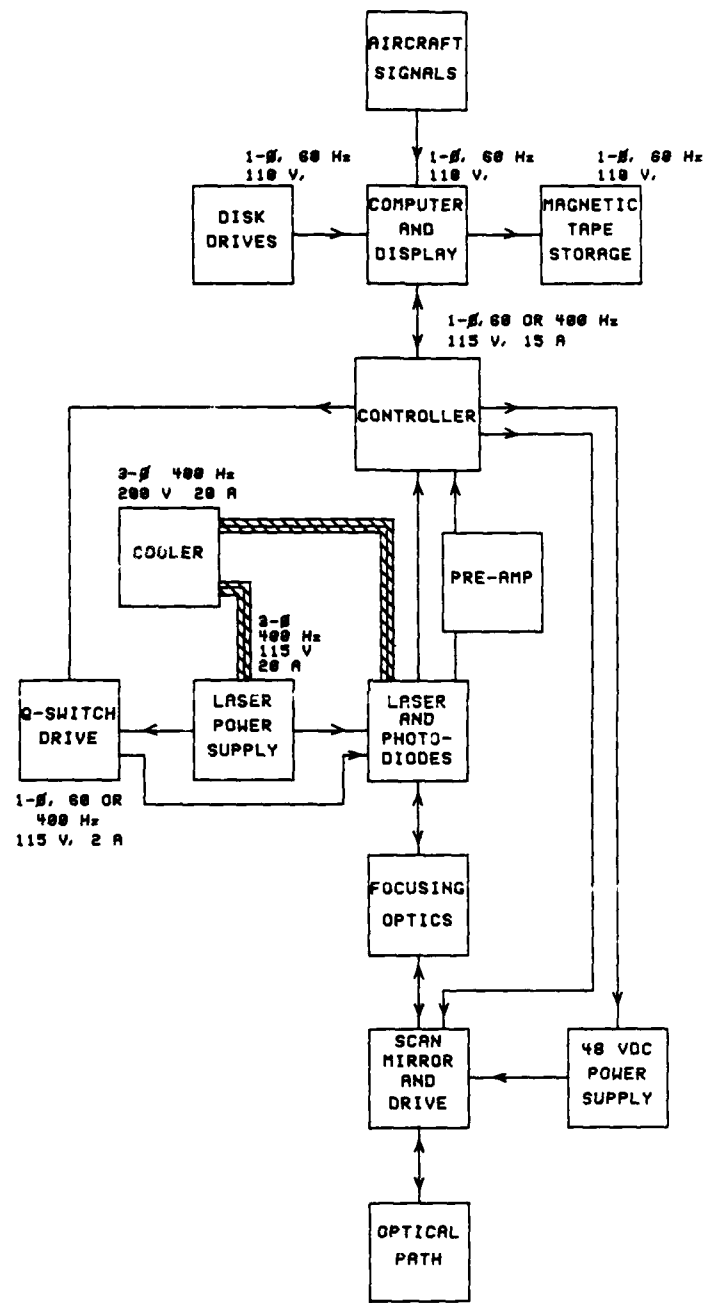


Figure 1. Block Diagram of OSRMS.

The display shows a speckled swath, brightest in the middle and falling off with a quasi-gaussian taper to darker edges. The width of the gaussian distribution depends on the ocean surface roughness: calm waters provide an extremely bright strip down the center with a sharp delineation to blackness at the sides, whereas very rough waters have an average intensity at the edges that is only slightly less than the center average. Superimposed on this pattern are the modulations of the internal waves. These are seen as bands of light and darker average intensities oriented at any angle through the swath.

The OSRMS is considered in greater detail in the following sections.

3. OSRMS Description

a) Mounting

A specially constructed frame contains the laser head, photodetectors, focussing optics, scan mirror, and the mirror drive motors and position sensors. This frame is positioned through the aircraft floor and bolted to the main aircraft I-beams. Two specially designed racks hold the rest of the OSRMS equipment, except for the computer system which is mounted in available space elsewhere in the aircraft.

It is desirable for the laser to be protected from shock on take-off and landing but rigidly coupled to the aircraft frame during operation. Removeable shock mounts are used for this purpose; they can be tightened down for rigid mounting or loosened for greater shock absorption, as needed. In the experiments the shocks were permanently tightened with no detrimental effect on the laser.

The computer hard-disk drive also requires special mounting. By construction, these devices are sensitive to vibration and tilt and require special consideration in the aircraft environment. In the experiments, the disk drive was mounted on a sheet of foam and tied down to a steel plate in

a rack to minimize vibration. To avoid operation while being tilted, the disk drive was used only to start up the system and the aircraft was flown straight and level during this time.

b) Electrical Requirements

The Convair 580 power supply has available 500 VA of three-phase 110 V at 60 Hz, 280 VA at 28 VDC, and 3 kVA of three-phase 110 V at 400 Hz. Figure 1 shows the OSRMS requirements.

The avalanche photodiode (APD) requires a low-current, high voltage, temperature-controlled bias of 300 V (nominal). This is generated from 28 V in circuitry housed with the preamplifier.

It should be noted that a 400 Hz power failure can be destructive with this particular laser because the laser head requires cooling during and for a time after operation or it may fracture internally. Therefore it is necessary to ensure that there is sufficient power available that normal fluctuations in the load will not cause the main breaker to trip.

Low voltages are also used and are produced within the OSRMS system by appropriate power supplies drawing 110 volts.

c) Electronics

Scan mirror control

The oscillations of the scan mirror cause the laser beam to trace out a swath on the ocean surface as shown in Figure 2.

A certain amount of aircraft pitch and roll can be accommodated so that the pattern on the ocean surface is not affected by reasonable flight variations. This is limited to ± 3 degrees of pitch and ± 5 degrees of roll centered around the nominal flying values of 2 degrees pitch, and 0 degrees roll at 200 knots ground speed.

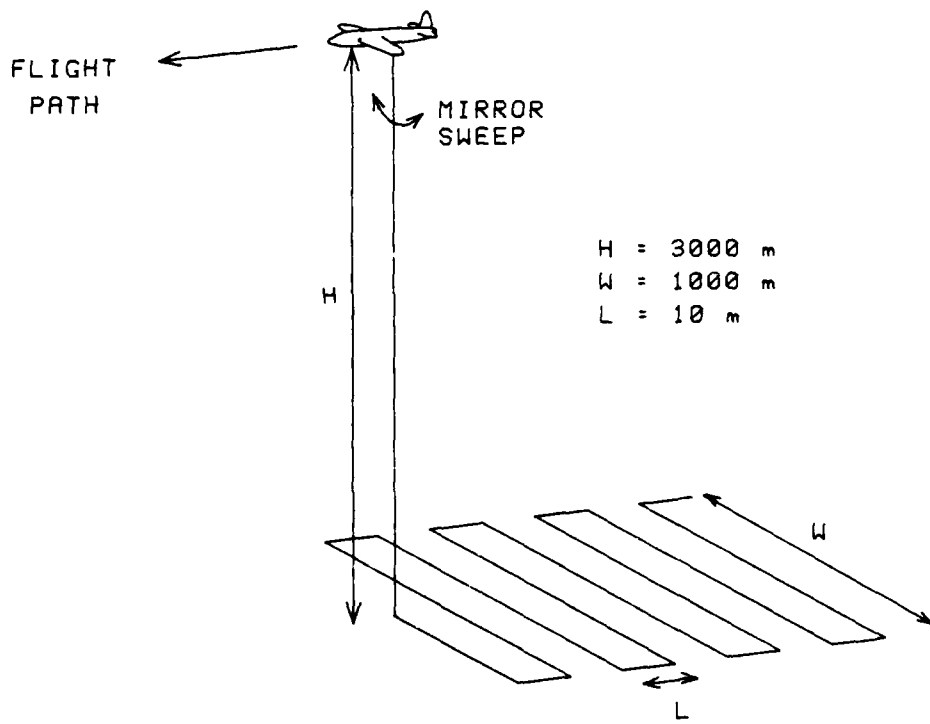


Figure 2. OSRMS Scan Pattern (not to scale).

The scan-mirror control section of the system comprises four cards of digital and analog integrated circuits: mirror sweep generator, mirror pitch control, mirror roll control, and laser fire control. These cards interface to the OSRMS computer for aircraft navigation data and to the motors which drive the scan mirror. Optical encoders and tachometers on the motor shafts provide feedback to the controller cards to ensure proper positioning of the scan mirror. Limit switches mechanically ensure that the system is shut down (scan-mirror servometers are disengaged and the laser-fire pulse is disabled) if the scan mirror is driven beyond its operating range.

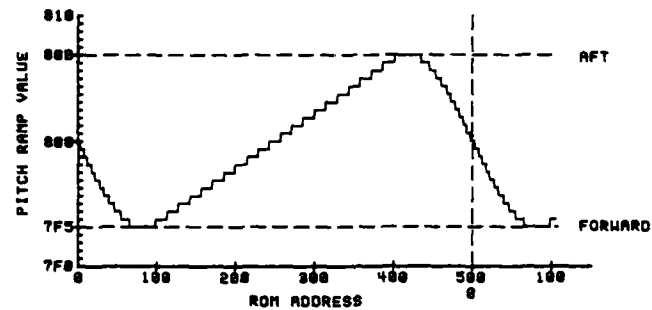
The scan pattern is produced through cooperation of the scan-mirror pitch and roll drives and the laser fire timing: at specific mirror positions the laser is pulsed by a trigger command from the controller. To determine the appropriate time for firing, the controller uses the "present" mirror position, the aircraft attitude data, and an optional manual offset input by the operator. The laser is fired one-hundred and one times across the swath to generate the basic transverse line of pixels. The mirror pitch control then "jumps" the mirror forward at the edge of the mirror scan, and when the mirror in its continuing roll oscillation is at the correct roll position, the laser begins a new set of one-hundred and one pulses scanning back across the swath in the opposite direction. The pulses are designed to be evenly spaced on the ocean surface, with the speed of the mirror scan and the laser fire frequency dependent upon the ground speed, and the center-to-center spacing between pixels dependent upon the aircraft height.

Computer interface

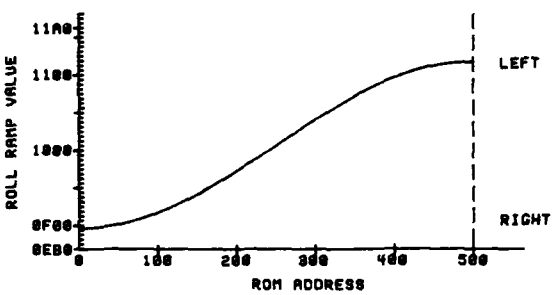
Aircraft pitch, roll and ground speed are sent from the computer to the controller. The laser fire control card contains the circuitry which receives, demultiplexes, and distributes the computer signal to the mirror sweep generator, the scan-mirror pitch control, and the scan-mirror roll control cards. The interface comprises 16-bit parallel data lines plus two control lines and one line carrying a reference voltage.

Mirror sweep generator

The aircraft ground speed is latched on the mirror sweep generator card and used to produce a train of clock pulses proportional to the ground speed. This clock signal drives counters which address the mirror pitch and roll programmable read-only memory (PROM) integrated circuits. The clock frequency is such that a total of five hundred memory locations are accessed during ten metres of aircraft travel. These PROMs thus produce the signals shown in Figure 3. These signals, referred to as



(a)
SCAN-MIRROR PITCH WAVE



(b)
SCAN-MIRROR ROLL WAVE

Figure 3. Scan-Mirror Drive Waveforms.

the scan-mirror pitch ramp and roll ramp, respectively, are multiplexed and displayed on the front panel of the controller and then are sent to the scan-mirror pitch and roll control cards respectively. There they are converted by the circuitry into forms necessary for driving the mirror motors and the resulting mirror movement causes the laser to trace out the desired pattern on the ocean surface. Because the width of the swath is dependent on the range of the firing angles and the aircraft altitude, different PROMs may be used for different altitudes to maintain the same swath width.

Scan-mirror pitch control

The pitch control card generates a value P_{DSP} , which represents the scan mirror's actual position in the pitch axis. It is the summation of the pitch encoder value from the position sensor on the pitch motor shaft, the aircraft pitch given by the computer, and the pitch offset value loaded by the operator at the front panel of the controller (which defaults to zero). The sum of P_{DSP} and the ramp produced by the mirror sweep generator card for pitch is converted to analog-form and added to the tachometer signal from the mirror-pitch motor shaft. This signal is filtered and sent to the motor to drive the scan mirror in the pitch direction.

Scan-mirror roll control

As in the pitch control card, the roll control card generates the value, R_{DSP} , for the scan mirror's actual position in the roll axis. It is the summation of the encoder value from the position sensor on the roll motor shaft, the aircraft roll given by the computer, and the roll offset value loaded by the operator at the front panel of the controller (which is normally zero). The position sensor on the roll axis motor shaft is only a relative positioning device producing pulses for movement, rather than producing a code representing absolute position (as is the encoder on the pitch axis). Extra circuitry is contained to add and subtract pulses to determine absolute position. The sum of R_{DSP} and the ramp produced by the mirror sweep generator card for roll is converted to analog-form, added to the tachometer signal from the mirror-roll motor shaft, and then fed through a bandpass filter to the motor which drives the scan mirror in the roll direction.

Laser fire control timing

The circuitry to control the timing of the laser pulses begins on the laser fire control card. The reset pulse (on power-up or reset) starts

the sequence: a counter addresses the PROM which contains the values corresponding to scan-mirror roll positions at which the laser should fire. When the PROM value equals the value of R_{DSP} calculated on the roll control card, indicating that the mirror is in the correct position, a laser trigger pulse is produced. This laser-fire pulse is sent also to the receiver card to start the timing chain which tells the receiver card when to expect signals from the laser photodetectors.

Receiver card

The infrared energy reflected from the ocean surface (the received pulse) is converted by the avalanche photodiode (APD) to electrical current, then amplified and converted to a voltage signal by the preamplifier at one of four possible gains chosen by the operator. This signal then goes to the receiver card.

The receiver card is housed in the controller. It is used to process the signals from the photodiodes which sense the amplitude of the outgoing laser pulse (i.e. the transmitted pulse) and the amplitude of the received pulse. Because the laser output varies from pulse to pulse, the transmitted values are used to normalize the received values to reduce the effect of this variation. The original design determined the transmitted pulse amplitude by directing part of the pulse through a fibre-optic delay line and back to the APD. The delay is necessary because the APD is saturated by scattered energy when the laser fires and takes some time to settle. This design was not satisfactory because excessive noise was introduced by the fibre-optic cable connections. In 1987 a p-i-n photodiode was attached at the back of the laser to sense directly the infrared pulse amplitude as the laser fires.

Preliminary signal analysis indicates that the normalization does not reduce noise in the signal in all cases. Possibly, under some circumstances nonlinearities in the response of the p-i-n diode or the APD (or both) become significant and require additional correction.

The transmitted and received signals are filtered and sent to a fast peak detector. The peak is sampled and converted to a 12-bit digital value which is then sent to the computer.

d) Computer System

The computer system comprises a Digital Equipment of Canada Ltd. (DEC) LSI-1173 computer with a video display, hard and floppy disk drives (Qualogy model 880 D30), and a Cipher Data Products Inc. Cache Tape, model number M890640-90-1000U, which is a 1600 bits-per-second, magnetic-tape storage system.

The system software is stored on a hard disk and contains the instructions for the computer system to interface the operator, the aircraft navigational system, and the OSRMS controller, to read and display data from all sources, and to store data for future use. The software is also designed to do as much real-time processing of the signals as possible.

The computer reads data from the aircraft navigation equipment and sends the pitch, roll, and ground speed to the controller for scan-mirror control. The controller returns the relative amplitudes of the transmitted and received laser signals.

The computer displays real-time data from the aircraft and the controller. The intensities of either the transmitted or received laser signals are displayed in a swath which corresponds to the one being traced out by the scan mirror. The display is scrolled up with new data added at the bottom of the screen as the old data are removed from the top. The display also gives information about the laser data including peak, minimum, and mean values, and standard deviation and standard error. These values are used by the software to optimize the display by adjusting the mapping of the range of amplitudes of the laser signals against the grey-scale range of

the monitor. The operator can also use these data to monitor the laser system for gain and drive current adjustments, etc. Navigational data and time are displayed also.

The data are written to magnetic tape at the end of each run.

e) Laser

The laser is a Control Laser Corporation krypton-lamp pumped Nd:YAG high-power 1.06 μm (infrared) laser, model number 514Q (modified), which includes a Q-switch to allow pulsed operation. The components and layout are shown in Figures 4 and 5.

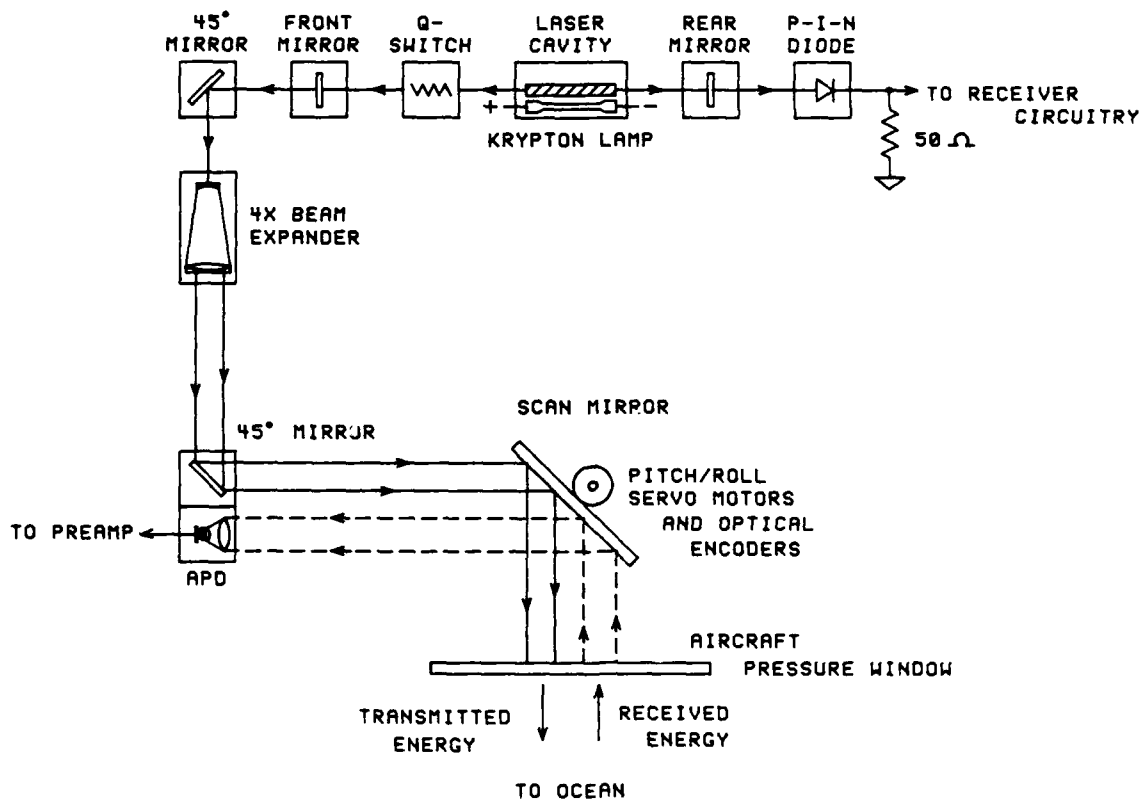


Figure 4. OSRMS Optical System Components.

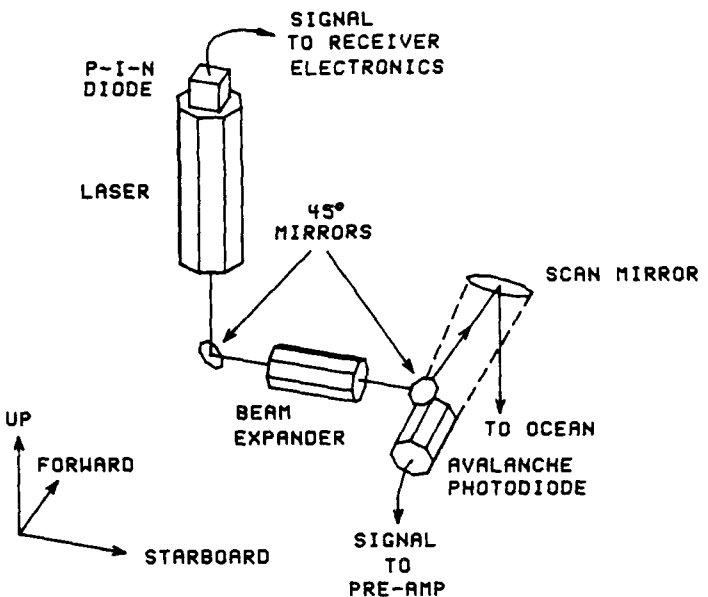


Figure 5. Optical System Layout (not to scale).

Once the laser beam passes through the laser's front aperture and partially reflective front mirror it is reflected from a gimballed adjustable beam-steering mirror to a beam expander which gives the beam the desired divergence angle. The alignment of the beam-steering mirror is critical in the performance, with small misalignments resulting in signal-to-noise ratios that are insufficient for reliable analysis of the data.

After the beam expander the beam is directed onto the center of the scan mirror by another carefully-aligned non-adjustable mirror. The scan mirror rotates about two axes, pitch and roll, which meet at its center, and directs the beam through the window in an access hatch in the underside of the fuselage. This window is specially coated to maximize the transmission of infrared radiation at $1.06 \mu\text{m}$ and allows a 19° field of view subtended from the center of the scan mirror.

Since infrared radiation is attenuated by water vapour, meaningful data cannot be collected unless the atmospheric path is free of cloud or heavy mist. Even moderately light mist, if variable, can cause unacceptable noise.

The energy reflected from the ocean surface which intercepts the scan mirror is reflected to the avalanche photodiode. The APD measures the amplitude of the infrared signal returned from the ocean surface. In the OSRMS system a temperature sensor is used to adjust the bias voltage across the diode to optimize its performance. The infrared signal is converted to a current by the APD, and then is amplified electrically and sent to the controller for processing.

Laser cooling

The cooling system used in the OSRMS is a modified Electro Impulse Inc. 2500 watt unit. It is a closed system circulating about 13 litres of deionized water through the laser head, the Q-switch, and the laser power supply. The heat is radiated to the air. The cooler is mounted in the power supply rack and has a particle filter and a deionizer in-line to keep the water clear of contaminants and ionization that could damage the laser head cavity.

Beam specifications

Table 1 shows the final beam diameters in two dimensions (x and y) for various lamp drive currents. The x-direction is across the swath and y is along the swath. The first five entries of each table show increasing lamp drive current with no adjustments made to the system. Because the beam becomes unstable at high drive amplitudes, the rear laser mirror was adjusted for stability, and measurements were repeated for 19.0 and 21.0 ampere drive currents. The beam diameter is calculated as being the width of the beam within which the intensity exceeds e^{-2} times the peak intensity of the spot.

It was preferred that the beam diameter be larger than ten metres rather than smaller because the beam intensity is not uniform and over-coverage has the advantage of better smoothing in the reflected signal. The

TABLE 1
BEAM SIZE VERSUS LASER CURRENT

| LASER CURRENT (AMPS) | PEAK DETECTOR VOLTAGE (VOLTS) | BEAM DIAMETER* | | | | | |
|----------------------------|--|---|--------|---|--------|---|--------|
| | | AT 55.0 FT (METERS) (X-AXIS) (Y-AXIS) | | AT 5500 FT (METERS) (X-AXIS) (Y-AXIS) | | AT 10,000 FT (METERS) (X-AXIS) (Y-AXIS) | |
| | | | | | | | |
| 17.0 | 0.210 | 0.0651 | 0.0599 | 6.510 | 5.987 | 11.836 | 10.884 |
| 18.0 | 0.235 | 0.0644 | 0.0616 | 6.444 | 6.165 | 11.717 | 11.209 |
| 19.0 | 0.240 | 0.0629 | 0.0650 | 6.290 | 6.500 | 11.435 | 11.819 |
| 20.0 ⁺ | 0.250 | 0.0724 | 0.0661 | 7.240 | 6.606 | 13.162 | 12.012 |
| 21.0 ⁺ | 0.255 | 0.0911 | 0.0723 | 9.113 | 7.227 | 16.571 | 13.139 |
| 19.0 [#] | 0.210 | 0.0806 | 0.0610 | 8.062 | 6.101 | 14.658 | 11.092 |
| 21.0 [#] | 0.170 | 0.1166 | 0.1176 | 11.656 | 11.760 | 21.194 | 21.382 |

* Beam diameter is defined as the beam width at an value of e^{-2} times the peak detector voltage. The measurements are made at 55 feet and extrapolated to 5500 and 10,000 feet.

⁺ The beam was multi-moding and unstable at these currents.

[#] The laser rear mirror was readjusted to produce a stable beam for these readings.

beam expander, therefore, was set to produce a spot size of at least ten metres at a distance of 10,000 feet with the minimum laser current to be used. The beam area, calculated from a histogram of intensity values as they occur within the beam, and plotted against laser drive current is shown in Figure 6. Here, the histogram is an ordering of intensities from maximum to minimum, and from it the number of intensity values containing a fraction of $1-e^{-2}$ of the total intensity "volume" integrated over the entire cross-section of beam values is used as the numerical value for beam area. For a Gaussian beam this fraction selects the contour with value e^{-2} times the maximum intensity and so for the general case it is somewhat equivalent to the Gaussian e^{-2} width. This approach circumvents the need to refer the

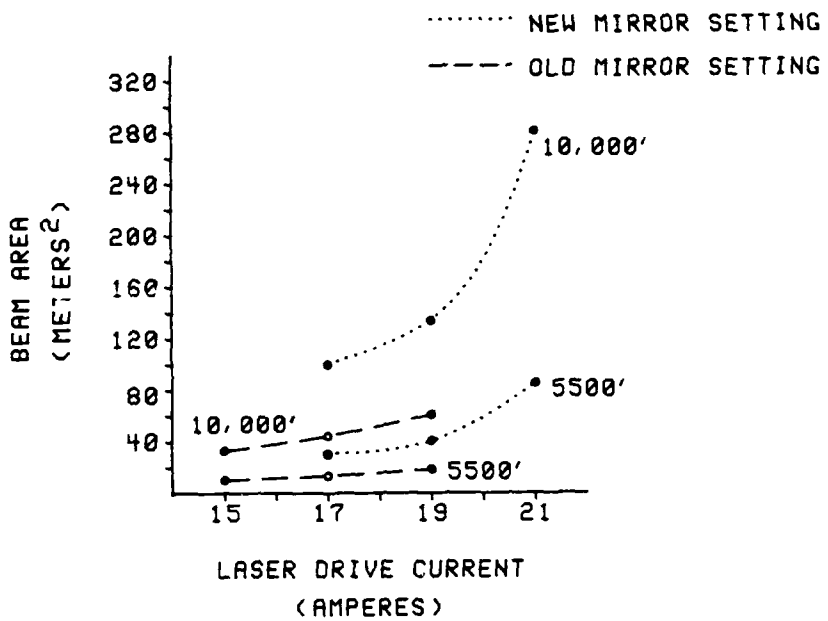


Figure 6. Beam Area Versus Drive Current.

contour to a peak value which may not be truly representative of the maximum beam intensity because of multimoding or noise. Symbolically, this process is given as follows. Let T be the total intensity "volume" within the beam. Then

$$T = \sum_{n=1}^N I_n * \Delta A$$

where I_n is the set of intensity values within the beam cross-section rank-ordered so that $I_1 > I_2 > I_3 > \dots > I_n$, and ΔA is the elemental area over which each I_n is measured. The total number of pixels discernibly illuminated is N . Then with $N_1 < N$ chosen so that

$$\sum_{n=1}^{N_1} I_n * \Delta A = (1 - e^{-2}) * T,$$

the beam area, A, is given by

$$A = N_1 * \Delta A$$

The numerical values of beam area are given in Table 2.

TABLE 2
BEAM AREA VERSUS LASER CURRENT

| LASER CURRENT (AMPS) | BEAM AREA* | |
|----------------------------|--------------------------------------|--|
| | AT 5500 FT (METERS ²) | AT 10,000 FT (METERS ²) |
| 15 ⁺ | 9.94 | 32.8 |
| 17 ⁺ | 13.4 | 44.4 |
| 19 ⁺ | 18.45 | 61.0 |
| 17 [*] | 30.2 | 100. |
| 19 [*] | 40.51 | 134. |
| 21 [*] | 85.3 | 281. |

* See text for method of calculation.

+ Laser mirror adjusted for JOWIP, SARSEX, and SCATMOD II.

* Laser mirror adjusted for SCATMOD III.

4. Review of Trials

a) Overview

JOWIP

The Joint Canada/US Ocean Wave Investigation Project^{2,3} (JOWIP) involved seven establishments in a two-and-one-half week trial in the summer of 1983. The trials took place over inshore waters adjacent to and in Georgia Strait near the Pacific coast. Two ships and five aircraft took part, and several different measurement systems were operated.

The main DREP objectives were to measure the transfer coefficients between internal wave surface currents and modulation depth in synthetic aperture radar⁴ (SAR) and OSRMS images⁵ and to compare the signal-to-noise ratios of these two systems. The results from this trial show clear internal wave modulations in the OSRMS signals⁵ although the transmitted energy levels were improperly recorded so that the results could not be normalized to remove the noise caused by pulse-to-pulse variations in the laser output.

SARSEX

The Synthetic-Aperture-Radar Signal Experiment⁶ (SARSEX) in the late summer of 1984 was organized to complete the objectives of JOWIP. Misalignment of the gimballed mirror in the OSRMS caused low signal-to-noise ratio and rendered its data unuseable.

Flights were made in the New York Bight area over naturally occurring oceanic internal waves. SAR images at L- and X-band were taken along with coincident surface and subsurface measurements, and for this instrument the noise level was low enough that internal wave signatures were clearly obtained and have been analyzed.^{7,8}

SCATTMOD II

This experiment took place during the late summer of 1985 in Georgia Strait near Nanoose, B.C. Many flights were taken over a three day period under wind conditions ranging from 2.2 m/s to 6.7 m/s. The NRC Convair 580 and the OSRMS, along with a helicopter for low-level aerial photography and an internal-wave-generating ship, were involved in the measurement series.

SCATTMOD III

In August of 1987 DREP carried out trials involving the NRC Convair 580 aircraft. The intent was to collect background noise data over open ocean waters by flying a star pattern with four legs separated in angle by 45 degrees over a predetermined location for several consecutive days. Unfortunately the weather during the trial period remained cloudy with very limited clear areas over the open ocean. Star-pattern measurements were taken where possible, as well as some wake measurements of freighters and some measurements over the Strait of Juan de Fuca and Georgia Strait. A summary of the runs is given in Table 3.

b) Data from SCATTMOD III

Most of the recordings taken over the West Coast show very little pattern modulation and minimal taper across the swath. The received data have been treated in various ways, namely, normalization by the transmitted pulse, removal of the taper by subtracting a cubic polynomial fitted across the swath to a mean calculated along the swath in the log domain, removal of "wild" points and interpolation of missing lines, and selection of acceptable portions of the data records, that is, those free from course corrections, large rolls or pitches, interference from clouds, etc. Three examples of the results of such treatment are given in Figures 7, 8, and 9.

TABLE 3
SUMMARY LOG OF SCATTMOD III RUNS

| DATE/TIME | MISSION/PASSES | COMMENTS |
|--------------|----------------|---|
| Aug 14/12:30 | 5/7 | Georgia Strait (Winchelsea Island to Comox B.C.): -nav system failure for part of mission |
| Aug 14/16:15 | 6/13 | Strait of Juan de Fuca (Race Rocks to near Sheringham Pt.): -some internal waves Georgia Strait (southern) -roll compensation testing -noise level testing |
| Aug 17/10:15 | 7/8 | Pacific ocean (48°45'N, 126°45'W): -star pattern -ship |
| Aug 17/15:10 | 8/10 | Pacific ocean (48°45'N, 126°45'W): -two ships sighted |
| Aug 18/11:00 | 9/8 | Pacific ocean: (48°16.9'N, 126°27.2'W): -mostly overcast, measurements made through a moving clear patch |
| Aug 18/15:00 | 10/8 | Pacific ocean: (48°31.4'N, 127°28.2'W): -clouds |
| Aug 19/10:45 | 11/11 | Pacific ocean: (48°45'N, 126°45'W): -no gyro signal -measurements at 5500 feet (under clouds) -some low clouds -natural internal waves -tanker and barge wakes |

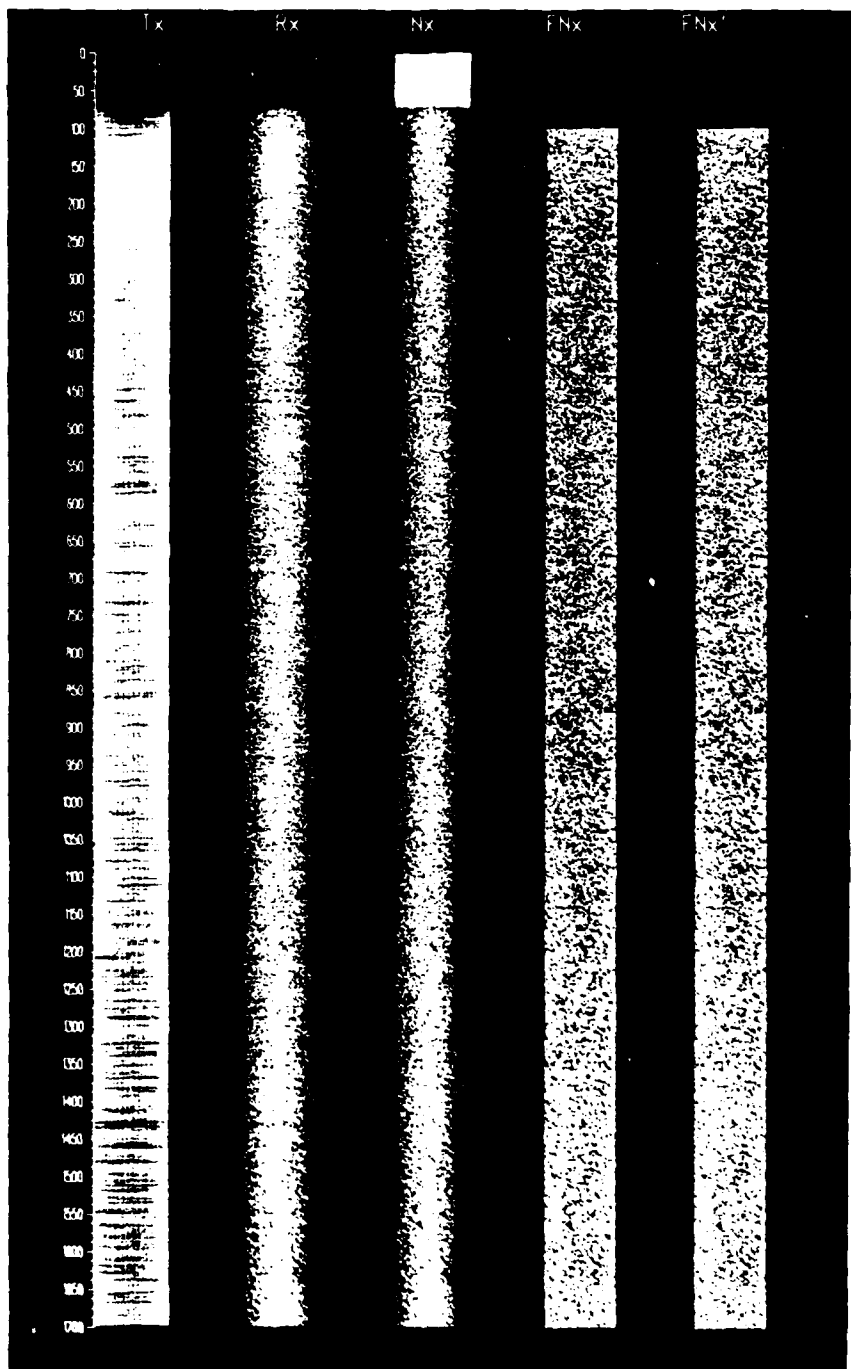


Figure 7. Example of OSRMS imagery taken on 1987 Aug 17, 11:32 to 11:35 at $48^{\circ}45'N$, $126^{\circ}45'W$. Wind speed is approximately 5-14 kts toward $040\text{-}060^{\circ}T$.

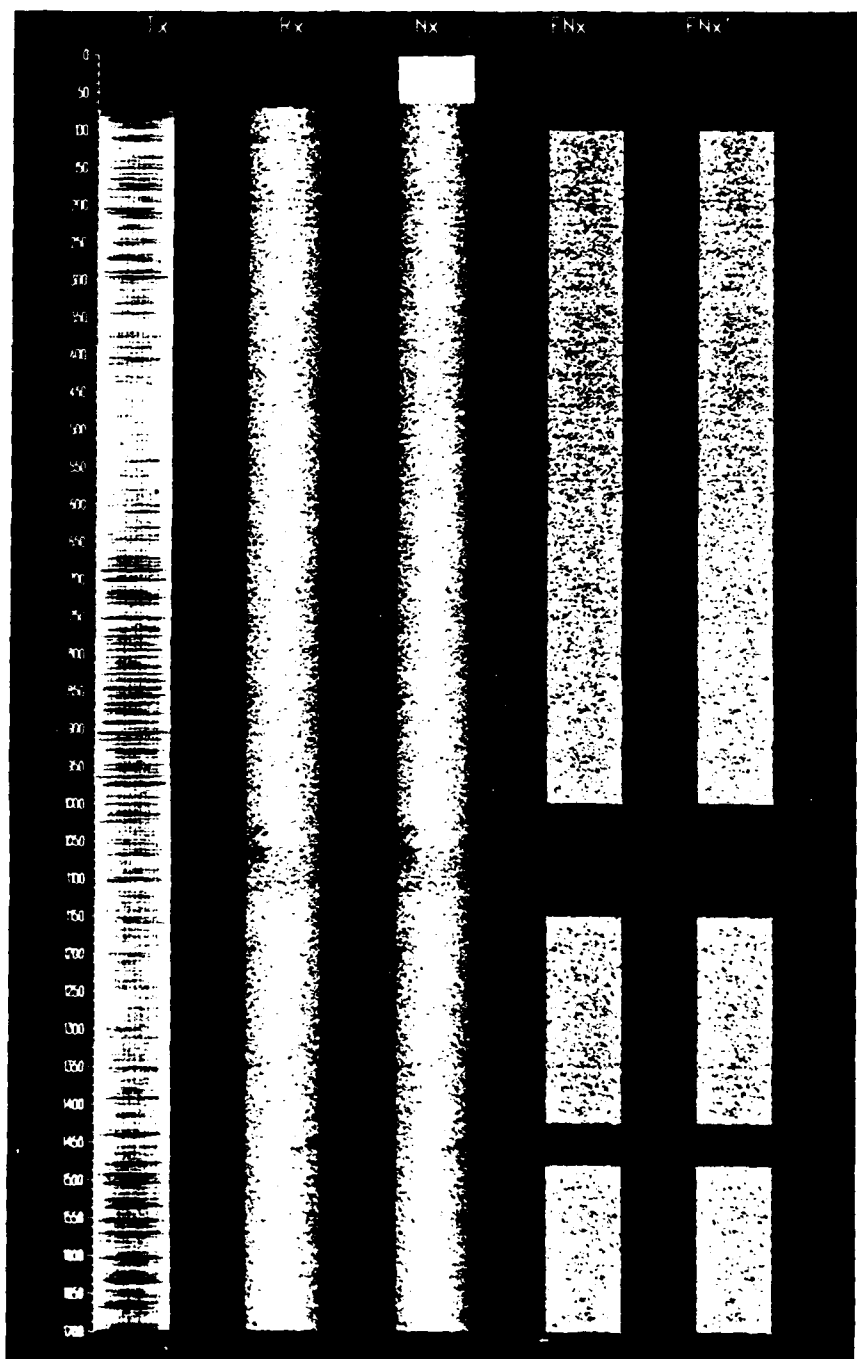


Figure 8. Example of OSRMS imagery taken on 1987 Aug 18, 11:12 to 11:15 at $48^{\circ}16.9'N$, $126^{\circ}27.2'W$. Wind speed is approximately 12 kts towards $045^{\circ}T$.



Figure 9. Example of OSRMS imagery taken at 1987 Aug 19, 12:05 to 12:08 at $48^{\circ}45'N$, $126^{\circ}45'W$. Wind speed is approximately 10 kts towards $090^{\circ}T$.

In all three figures the transmitted signal (Tx) displays a cross-hatched pattern composed of a vertical line structure and superimposed horizontal streakiness. This pattern occurs commonly, and the vertical lines (in the figure) are probably due to the fixed but uneven pattern in the timing between successive pulse firings allowing the Q-switched laser cavity to "charge" for different lengths of time.

The taper across the received swath (Rx) is apparent in Figures 7 to 9 as well. The normalized received swath (Nx) also displays the taper. Unuseable swath portions have been removed from the two right-most columns (FNx, FNx'), for example, Figure 8 lines 0-75, 1000-1150, 1420-1470, the last two of which are darkenings due to clouds. In the FNx column the mean taper has been removed and in FNx' the standard deviation also has been made uniform across the swath to remove the residual effect of the taper that remains in the speckle noise.

Internal waves were also encountered and an example is shown in Figure 10. The internal waves are apparent in the four right-hand swaths (Rx-FNx') at 650-850 and they show up primarily as extra whiteness in the speckled grey background. The scan line spacing here is 5.5 m and so these 200 scan lines represent 1.1 km. The dark lines near line 100 and the white lines between 1160 and 1270 may also be representations of internal waves.

During the course of the measurements several freighter wakes and smaller ship wakes also were encountered, and examples are shown in Figures 11 and 12. The former is the wake of the freighter FRUITION encountered 19 August on a heading of 098°T in a wind of 5 m/s blowing towards 090°T. The FRUITION's speed was 7 m/s. Other ships that were encountered were undocumented.

In Figure 11 the FRUITION is just above the top of the receive swath and the left edge of its turbulent wake is visible as the whitish "scar" running the whole length of the visible swath. With a scan line

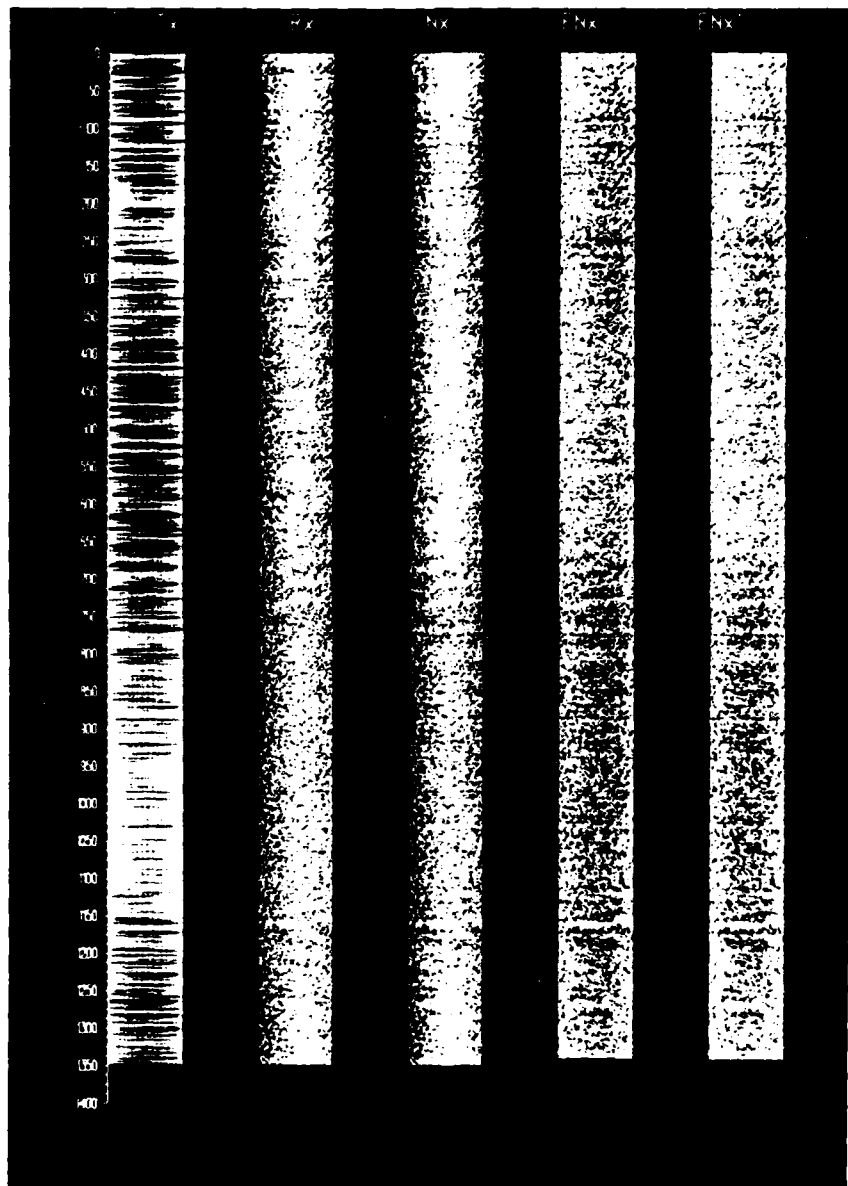


Figure 10. OSRMS image showing internal wave modulation. Taken at 1987 Aug 19, 12:52 to 12:55, at $48^{\circ}45'N$, $126^{\circ}45'W$.



Figure 11. OSRMS image showing the wake of the freighter FRUITION. Taken on 1987 Aug 19, 12:28 to 12:31, at $48^{\circ}45'N$, $126^{\circ}45'W$. The wind is 5 m/s towards $090^{\circ}T$ and the freighter's speed is 7 m/s.



Figure 12. Example of an undocumented ship wake taken on 1987 Aug 17,
16:13 to 16:16 at 48°45'N, 126°45'W.

spacing of 5.5 m this represents a wake length of approximately 8 km. Figure 12 clearly shows a small ship at line 1200 with a wake extending visibly to about line 1350. Natural internal waves are also visible between lines 1000 and 1300. Here the scan line spacing is 10 m.

Tests were made of the effectiveness of the OSRMS compensation for aircraft roll. A small uncorrected residual still remains, possibly phase shifted from the main roll component, but the major portion of the roll is properly compensated. Examples of compensated and uncompensated image portions taken when the aircraft was executing rolls of 6 to 10 degrees are shown in Figure 13. From line 0 to line 400 straight and level flight was maintained over calm water. The main reflections in the swath are confined to a very narrow strip centered vertically below the aircraft. For the next 1000 lines the aircraft executed roll manoeuvres with the roll compensation turned off until line 1080 and then turned on for the rest of the swath length (until line 1400). The reflected energy is registered in a coordinate frame fixed to the OSRMS (i.e. the aircraft), then as the aircraft rolls, the position of vertical shifts across the swath accordingly. It can be seen that only a small residual uncompensated portion of the roll remains after the compensation is applied.

Static calibration measurements showing infrared beam angle with respect to the aircraft as a function of roll ramp value (as fed in manually to the OSRMS) are shown in Figure 14. The linearity is excellent.

Finally, image intensity standard error (speckle standard deviation/mean) is shown as a function of wind orientation and speed in Figure 15. The data used are from the star patterns flown over the open ocean with the sections showing cloud absorption, internal waves, or ship wakes removed. Also, because the intensity taper inherent in the measurement increases the noise of the standard error, only the central 16 pixels in each swath are used. The standard error of the remaining data was

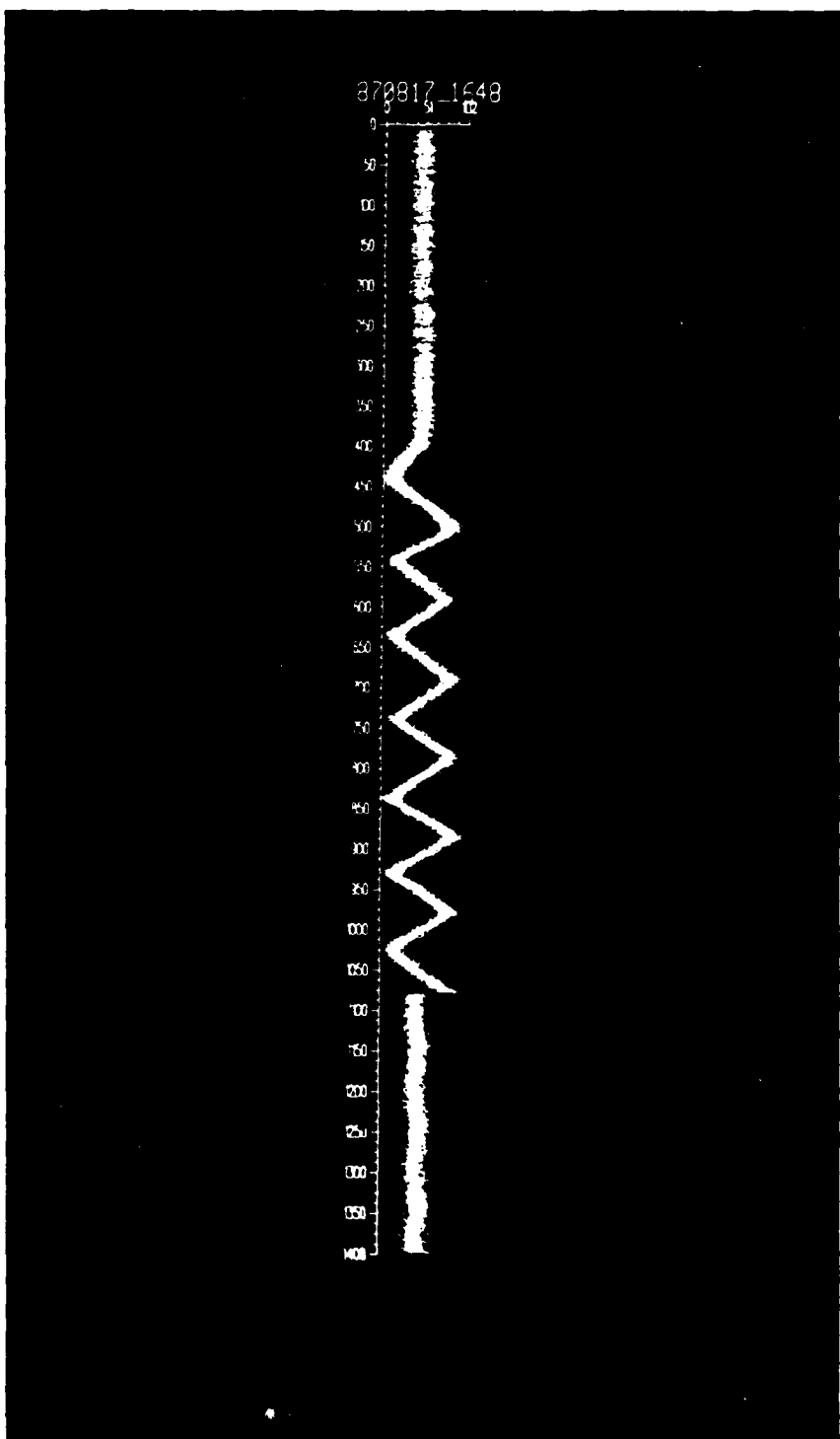


Figure 13. Imagery showing effect of roll compensation.

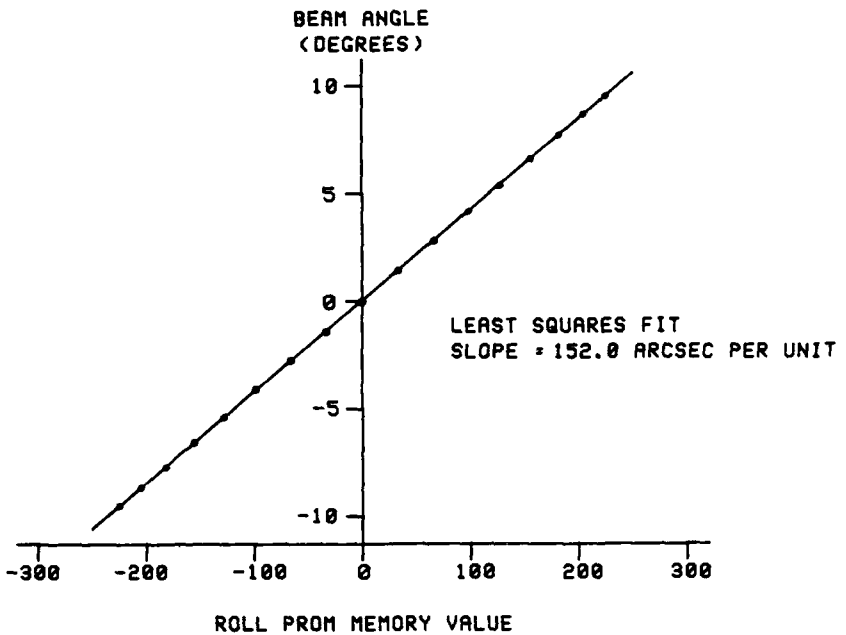
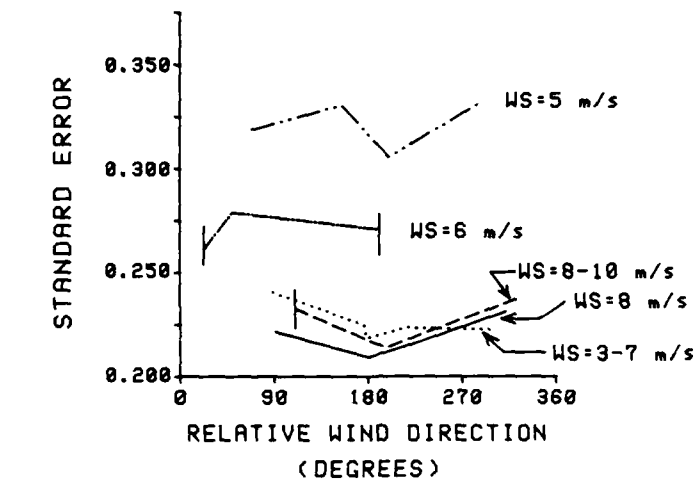
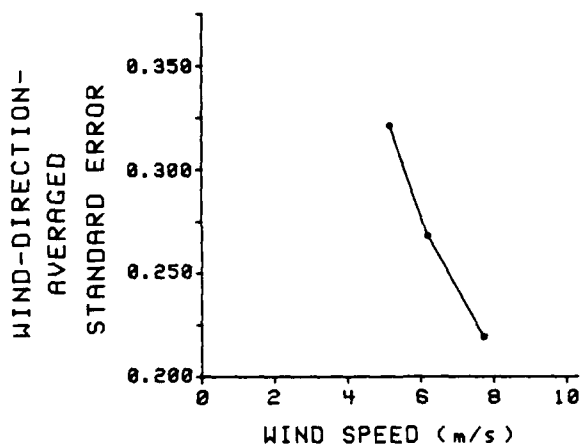


Figure 14. Beam Angle Versus Roll Ramp.

calculated and is plotted against the relative wind direction⁹ in Figure 15a. The relative wind direction here is defined as the angle between the aircraft heading and the direction to which the wind is blowing. The small vertical bars on the 6 m/s and 8-10 m/s lines indicate the range of several data points that were coincident in wind direction. The lines are drawn through the averages.



(A)



(B)

Figure 15. Standard Error Versus Wind Direction and Speed.

The standard errors are all considerably higher than those measured in Georgia Strait with a single spot scatterometer.¹⁰ Under the conditions of those measurements, the standard error for a beam of 2.5 m radius (corresponding to 19 amperes at 5500 feet, Table 1, with the effective radius given by beam diameter/2/2) ranged from 0.1 to 0.25. This beam radius corresponds to the conditions of only the left-most data point in the WS-5 m/s curve in Figure 15a. The rest of the 5 m/s curve and all but the right-most point in the 3-7 m/s curve have effective beam radii of about 4 m. All the others are 7.5 m radii. At 7.5 m the previously measured data predicts standard errors of 0.06 to 0.14, much less than all of the data measured here. The increased standard errors in the present data set and the apparent sensitivity of the standard errors to effective beam radius may indicate the presence of residual long-wavelength modulation on the sea surface.

A direct measure of beam radius effect can be seen near 180° in the 3-7 m/s line (dotted) in Figure 15a. The downturn is caused by a data point at 176° with a standard error of 0.229, taken with an effective beam radius of 4.5 m, and one at 178° with a standard error of 0.223, and a beam radius of 7.5 m. The previous data set¹⁰ would indicate an expected change of 40% whereas the present data has changed by only 3%.

There also seems to be very little systematic wind-direction effect in the standard error. The standard error averaged over all relative wind directions for each wind speed (the "wind-direction-averaged standard error") is plotted against wind speed in Figure 15b. Only the three sets of data with non-variable wind speed are included. These data show a decrease in average standard error for increasing wind speed.

5. Conclusions

The OSRMS is shown to be capable of taking quantitative measurements of ocean surface roughness parameters over a 1000-metre swath

at 200 knots aircraft speed. While tests show that the equipment functions very well (for example, the roll compensation circuitry and the beam angle versus roll ramp linearity), areas for potential improvement still remain (hard-disk-drive problems and system noise). Also the weather-related limitations of this system are clearly evident. Data collected clearly show internal waves, ship wakes, and wind speed effects.

The speckle noise level for data taken in open ocean conditions under moderate wind speeds is larger than that predicted by previous measurements in inshore waters.

REFERENCES

1. Hershtal Z., "Ocean Surface Roughness Measurement System: Phase I Final Report", DREP Contractor's Report Series 83-2, May 1980.
2. Hughes B.A., S.J. Hughes, T.W. Dawson, "Joint Can/US Ocean Wave Investigation Project, Objectives, Procedures and Description of DREP Data for the Georgia Strait Experiment (July/August 1983)", DREP Technical Memorandum 84-7, September 1984.
3. Hughes B.A. and T.W. Dawson, "Joint CAN/US Ocean Wave Investigation Project (JOWIP), the Georgia Strait Experiment: An Overview", accepted for publication in J. Geophys. Res.
4. Hughes S.J. and B.A. Hughes, "Estimation of Internal Wave Surface Currents from SAR Imagery", DREP Report 87-1, March 1987.
5. Hughes S.J. and B.A. Hughes, "Estimation of Internal Wave Currents from SAR and Infrared Scatterometer Imagery", Proc. IGARSS'86 Symposium, Zurich, ESA SP-254, pp. 789-794, August 1986.
6. Sarsex Experiment Team, "Sarsex Interim Report", JHU/APL STD-R-1200, John Hopkins University Applied Physics Laboratory, May 1985.
7. Gasparovic R.F., J.R. Apel, and E.S. Kasischke, "An Overview of the SAR Internal Wave Signature Experiment", accepted for publication in J. Geophys. Res.
8. Thompson D.R. and R.F. Gasparovic, "Intensity Modulation in SAR Images of Internal Waves", Nature, 320, 345-348, 1986.

9. The wind directions and speeds used were obtained from METOC, MARPAC, CFB Esquimalt.
10. Hughes B.A. and S.J. Hughes, "Measured Ocean Speckle Noise for a Nadir-Looking Near-Infrared Scatterometer", DREP Report 83-5, October 1983.

REPORT NO: DREP TECHNICAL MEMORANDUM 88-15
TITLE: OSRMS: The DREP Near-Nadir Scatterometer
AUTHORS: L.C. Rempel, B.A. Hughes and S.J. Hughes
DATED: August 1988
SECURITY GRADING: UNCLASSIFIED

3 - DSIS

Circulate to:
DRDM
DSP

1 - DREV

1 - DREO
1 - DREA

1 - DGAEM

1 - DAR

1 - DGMEM

1 - DGIS/DSTI

1 - ORAE Library

1 - D Met Oc

1 - Maritime Tech Library

1 - Bedford Inst of Oceanography
Library

1 - NRC

1 - RRMC Dept of Oceanography

1 - RMC

1 - CFMWS

1 - CRC Library

1 - CDLS(L) CDR

1 - CDLS(W) CDR

1 - DRA Paris

1 - Commander

Maritime Command

Attn: MC/ORD

1 - SSO OpRsCh/MARPAC

1 - RADARSAT Office

110 O'Connor St., Suite 200
Ottawa, ON K1P 5M9
Attn: Mr. Ed Langham

1 - Canada Centre for Inland Waters

Burlington, ON L7R 4A6
Attn: Mr. Mark A. Donelan

1 - RESORS

Canada Centre for Remote Sensing
240 Bank Street, 5th Floor
Ottawa, ON K1A 0Y7
Attn: Mr. G. Thirlwall

AUSTRALIA

1 - Surveillance Systems Group

Electronics Research Laboratory
G.P.O. Box 2151
Adelaide, S. Australia 5001
Attn: Dr. D. Cartwright

BRITAIN

1 - Ministry of Defence

1 - DRIC

1 - Thomas Hennessy

Admiralty Research Establishment
Queen's Road, Teddington
Middlesex TW11 0LN
England

DISTRIBUTION (continued)

UNITED STATES

- 3 - DTIC
1 - Naval Research Laboratory
Washington, D.C. 20375
1 - Environmental Research Inst.
of Michigan
P.O. Box 8618
Ann Arbor, Michigan 48107
Attn: Dr. R. Shuchman
- 3 - Applied Physics Laboratory
Johns Hopkins Road
Laurel, MD 20707
1 - Dr. R. Gasparovic
1 - Dr. B. Gotwols
1 - Dr. D. Thompson
- 2 - Naval Ocean Systems Center
San Diego, CA 92152
1 - Dr. R.R. Buntzen
1 - Dr. R.R. Hammond
- 2 - TRW Inc.
1 Space Park
Redondo Beach, CA 96278
1 - Dr. B. Lake
1 - Dr. D. Kwoh
- 1 - Dynamics Technology Inc.
22939 Hawthorne Blvd.
Suite 200
Torrance, CA 90505
Attn: Dr. M. Dube
- 1 - Dynamics Technology Inc.
1815 N. Lynn St.
Suite 810
Arlington, VA 22209
Attn: Dr. S. Borchardt
- 1 - Dr. R.S. Winokur
Assoc. Technical Director for
Ocean Science and International Proc.
Office of Naval Research
Arlington, VA 22217
- 1 - Defense Advanced Research
Projects Agency
1400 Wilson Blvd.
Arlington, VA 22209
- 1 - R.D. Associates
P.O. Box 9695
Marina Del Rey, CA 90291
Attn: Dr. D. Holliday
- 1 - Institute of Geophysics and
Planetary Physics, A-025
Scripps Institution of Oceanography
La Jolla, CA 92093
Attn: Prof. W. Munk
- 1 - Science Applications Inc.
1200 Prospect St.
P.O. Box 2351
La Jolla, CA 92038
- 1 - Applied Physics Technology, Inc.
1800 Old Meadow Rd., #1015
McLean, VA 22102
Attn: Dr. C.V. Swanson
- 1 - Dr. Arthur Reed
9106 Warren St.
Silver Spring, MD 20910
- 1 - Dr. D. Lyzenga
College of Marine Studies
University of Delaware
Newark, Delaware 19716

UNCLASSIFIED

SECURITY CLASSIFICATION OF FORM
 (Highest classification of Title, Abstract, Keywords)

DOCUMENT CONTROL DATA

(Security classification of title, body of abstract and indexing annotation must be entered when the overall document is classified)

| | | |
|--|---|--|
| 1. ORIGINATOR (the name and address of the organization preparing the document Organizations for whom the document was prepared, e.g. Establishment sponsoring a contractor's report, or tasking agency, are entered in section 8.) Defence Research Establishment Pacific Forces Mail Office Victoria, B.C. V0S 1B0 | | 2. SECURITY CLASSIFICATION (overall security classification of the document including special warning terms if applicable) UNCLASSIFIED |
| 3. TITLE (the complete document title as indicated on the title page. Its classification should be indicated by the appropriate abbreviation (S,C,R or U) in parentheses after the title.) OSRMS: The DREP Near-Nadir Scatterometer. | | |
| 4. AUTHORS (Last name, first name, middle initial) Rempel, L.C., Hughes, B.A., and Hughes, S.J. | | |
| 5. DATE OF PUBLICATION (month and year of publication of document) August 1988 | 6a. NO. OF PAGES (total containing information. Include Annexes, Appendices, etc.) | 6b. NO. OF REFS (total cited in document) 12 |
| 7. DESCRIPTIVE NOTES (the category of the document, e.g. technical report, technical note or memorandum. If appropriate, enter the type of report, e.g. interim, progress, summary, annual or final. Give the inclusive dates when a specific reporting period is covered.) Technical Memorandum | | |
| 8. SPONSORING ACTIVITY (the name of the department project office or laboratory sponsoring the research and development. Include the address.) DREP | | |
| 9a. PROJECT OR GRANT NO. (if appropriate, the applicable research and development project or grant number under which the document was written. Please specify whether project or grant) DRDM-04 | 9b. CONTRACT NO. (if appropriate, the applicable number under which the document was written) | |
| 10a. ORIGINATOR'S DOCUMENT NUMBER (the official document number by which the document is identified by the originating activity. This number must be unique to this document) TM 88-15 | 10b. OTHER DOCUMENT NOS. (Any other numbers which may be assigned this document either by the originator or by the sponsor) | |
| 11. DOCUMENT AVAILABILITY (any limitations on further dissemination of the document, other than those imposed by security classification) <input checked="" type="checkbox"/> Unlimited distribution <input type="checkbox"/> Distribution limited to defence departments and defence contractors; further distribution only as approved <input type="checkbox"/> Distribution limited to defence departments and Canadian defence contractors; further distribution only as approved <input type="checkbox"/> Distribution limited to government departments and agencies; further distribution only as approved <input type="checkbox"/> Distribution limited to defence departments; further distribution only as approved <input type="checkbox"/> Other (please specify): _____ | | |
| 12. DOCUMENT ANNOUNCEMENT (any limitation to the bibliographic announcement of this document. This will normally correspond to the Document Availability (11). However, where further distribution (beyond the audience specified in 11) is possible, a wider announcement audience may be selected.) _____ | | |

UNCLASSIFIED

SECURITY CLASSIFICATION OF FORM

UNCLASSIFIED

SECURITY CLASSIFICATION OF FORM

13. ABSTRACT (a brief and factual summary of the document. It may also appear elsewhere in the body of the document itself. It is highly desirable that the abstract of classified documents be unclassified. Each paragraph of the abstract shall begin with an indication of the security classification of the information in the paragraph (unless the document itself is unclassified) represented as (S), (C), (R), or (U). It is not necessary to include here abstracts in both official languages unless the text is bilingual).

→ The ocean surface roughness measurement system (OSRMS) is a near-nadir-directed infrared (IR) scatterometer, specially constructed for and operated by the Defence Research Establishment Pacific (DREP). It has been used to measure ocean-surface parameters and particularly for the examination from an aircraft of internal waves.

This paper gives a description of the configuration and operation of the OSRMS including the mechanical, electrical, electronic, optical, and software components. A brief overview of the trials in which the OSRMS took part is included, with the main focus on the 1987 trial, SCATTMOD III and the data obtained in that trial. The discussion of the data from this trial contains examples of internal waves, ship wakes, and aircraft attitude compensation, and a description of wind velocity effects on the speckle noise.

Key words

14. KEYWORDS, DESCRIPTORS or IDENTIFIERS (technically meaningful terms or short phrases that characterize a document and could be helpful in cataloguing the document. They should be selected so that no security classification is required. Identifiers, such as equipment model designation, trade name, military project code name, geographic location may also be included. If possible keywords should be selected from a published thesaurus, e.g. Thesaurus of Engineering and Scientific Terms (TEST) and that thesaurus-identified. If it is not possible to select indexing terms which are Unclassified, the classification of each should be indicated as with the title.)

→ Remote sensing,
Scatterometer,
Internal wave,
Laser,
Infrared,
Ocean Roughness. Canada.

UNCLASSIFIED

SECURITY CLASSIFICATION OF FORM